Monatsh Chem (2014) 145:1201–1211
DOI 10.1007/s00706-014-1212-y

ORIGINAL PAPER

Insights into mechanism of anticancer activity of pentacyclic oxindole alkaloids of *Uncaria tomentosa* by means of a computational reverse virtual screening and molecular docking approach

Paweł Kozielewicz · Katarzyna Paradowska · Slavica Erić · Iwona Wawer · Mire Zloh

Received: 9 March 2014 / Accepted: 23 March 2014 / Published online: 24 May 2014

Abstract Alkaloid-rich extract from *Uncaria tomentosa* (cat's claw) has been reported to cause apoptosis in cancer lines. Oxindole pentacyclic alkaloids of the plant are responsible for this effect, yet their biological mechanism of action is not fully understood. In this work the set of these alkaloids underwent an extensive theoretical study with reverse virtual screening and molecular docking methods implemented in AutoDock, AutoDock Vina, and Molegro Virtual Docker. The results from these computational methods indicate that inhibition of several important targets including dihydrofolate reductase and mouse double minute 2 homolog (MDM2) may be responsible for the biological activity of the alkaloids. The docking results also show that the alkaloids can interact with Dvl-2, Akt-2, and leukotriene A4 hydrolase. Reverse virtual screening and molecular docking are valuable tools to aid identification of protein targets for bioactive hit molecules and could guide the design of in-depth biochemical activity tests and utilization of these alkaloids in anticancer drug development.

Keywords Apoptosis · Molecular docking · Reverse virtual screening · Oxindole alkaloids · *Uncaria tomentosa*

Introduction

Uncaria tomentosa (cat's claw) is a woody vine from the Peruvian Amazon. The bark, roots, and leaves of this plant have been used in traditional medicine by the native people of Peru since the Incas to treat a wide range of illnesses, such as diarrhea, rheumatic and gastrointestinal disorders, cancer, diabetes, and acne [1]. Traditionally, decoctions of *U. tomentosa* were prepared from roots and bark. The chemical profile of the plant constituents is diversified. The extracts of *U. tomentosa* bark contain quinovic acid glycosides, triterpenes, flavonoids (rutin and quercetin), phytosteroids (β-sitosterol, stigmasterol, and campesterol), and catechins. However, the most valuable chemicals are tetra- and pentacyclic oxindole and indole alkaloids. Two chemotypes of *U. tomentosa* have been established: one containing mainly pentacyclic, and the other containing tetracyclic indole and oxindole alkaloids in various parts of the plant [2].

Among the tetracyclic alkaloids, isorhynchophylline and rhynchophylline were proved to be *N*-methyl-D-aspartate (NMDA) receptor antagonists and Ca^{2+} channel blockers [3]. Furthermore, pentacyclic alkaloids have been reported to exhibit antiproliferative effects via stimulation of apoptosis [4–6]. In the past, we studied these compounds

Electronic supplementary material The online version of this article (doi:10.1007/s00706-014-1212-y) contains supplementary material, which is available to authorized users.

P. Kozielewicz (✉)
School of Clinical and Experimental Medicine, College of Medical and Dental Sciences, University of Birmingham, Edgbaston, Birmingham B15 2TT, UK
e-mail: p.kozielewicz@pgr.bham.ac.uk

K. Paradowska · I. Wawer
Faculty of Pharmacy, Medical University of Warsaw, Banacha 1, 02-097 Warsaw, Poland

S. Erić
University of Belgrade-Faculty of Pharmacy, Vojvode Stepe 450, 11000 Belgrade, Serbia

M. Zloh
Department of Pharmacy, University of Hertfordshire, Hatfield, Hertfordshire AL10 9AB, UK

by means of nuclear magnetic resonance (NMR) and gauge including atomic orbitals-density functional theory (GIAO-DFT) methods [7]. The chemical structures of these pentacyclic compounds are presented in Fig. 1.

Despite a growing number of reports describing the clinical and biological effects of *U. tomentosa* extracts, its pharmacological proapoptotic effectiveness and molecular targets are largely unknown. It was suggested that pentacyclic oxindole alkaloids, which are the key components responsible for the proapoptotic effect of the extract, can act through different mechanisms. According to Berry et al. [8], alkaloids act as inhibitors of protein tyrosine kinase. The authors of the study suggested that the alkaloids' mode of action is a consequence of similarity between the oxindole fragment in their structure and the indole part of adenosine triphosphate (ATP). Alkaloid extracts were tested on breast and skin carcinoma cell lines and exhibited antiproliferative activity with 50 % inhibition concentration (IC_{50}) from 0.9 to 1.7 mM. In the study by Gurrola-Diaz et al. [5] a link was suggested between the alkaloids' activity and the Wnt signaling pathway. Aqueous and alkaloid-enriched extracts of *U. tomentosa* exhibited downstream regulation on the Wnt signaling pathway in HeLa, HCT116, and SW480 cancer cells, resulting in reduced expression of the Wnt target gene. Another possibility is activation of caspase 3, which was suggested by De Martino et al. [4]. Western blot analysis showed an increased rate of procaspase 3 cleavage leading to caspase 3 activation in HeLa cells comparable to the activation after etoposide administration. The paper presented by Hardjito et al. [9] states that one of the alkaloids, isopteropodine, can interact with topoisomerase I. The activity to inhibit topoisomerase I [represented by the minimum inhibitory concentration (MIC) value] was measured by the method described by TopoGEN and for methanol extract was 2.5 μg/cm^3. The authors were not certain, however, that this alkaloid is the responsible inhibitor, as other active compounds may exhibit this property, including fulvoplumierin. Pilarski et al. [10] used alkaloid-enriched extract to treat HL60 cells. They subsequently suggested that alkaloids inhibit nuclear factor kappa-light-chain-enhancer of activated B cells (NF-κB). Recently, studies of antineoplastic effects of an *Uncaria tomentosa* (UT) raw hydroethanolic extract [11] indicated that modulation of oxidative stress by synergistic activity of different classes of chemical compounds could be a

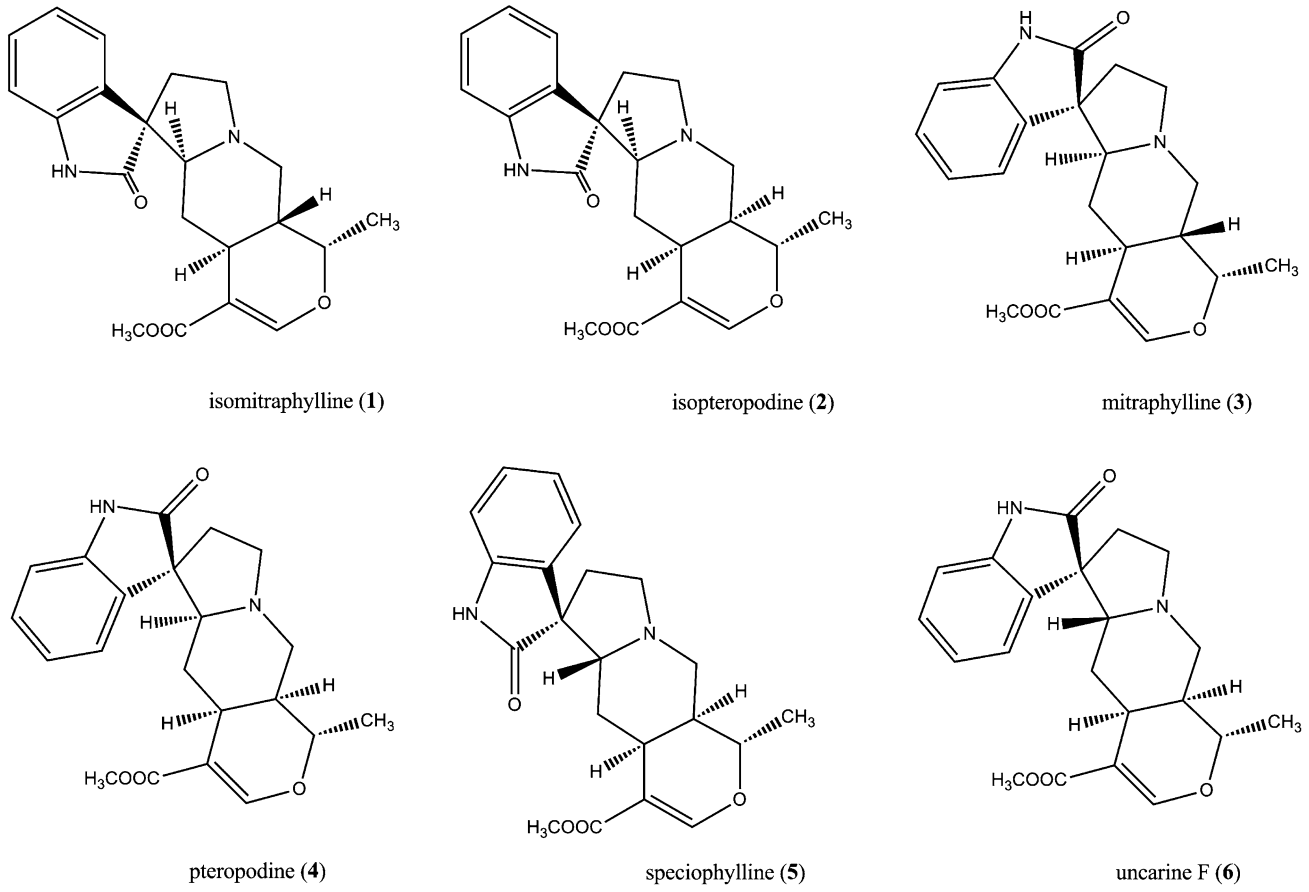

Fig. 1 Molecular structures of pentacyclic oxindole alkaloids of *U. tomentosa*

main reason for tumor growth inhibition. These studies still did not reveal the mechanism of action of the oxindole pentacyclic alkaloids.

Reverse virtual screening provides users with screening for potential targets of known ligands. TarFisDock [12] and ReverseScreen3D [13] are online servers that offer the possibility to screen compounds against large numbers of molecular targets. Recently, we demonstrated successful target identification for a series of aryl-aminopyridines by use of a combination of TarFisDock and targets found by literature search [14]. TarFisDock explores the interaction of studied ligands with a chosen pool of potential targets using a molecular docking approach. This online tool generates a set of possible targets, and results then should be examined in a careful manner and correlated with experimental data. On the other hand, ReverseScreen3D takes into consideration the similarity between ligands extracted from crystal structures and the ligands in a query.

Our goal is to find a few most possible molecular targets for alkaloids using theoretical methods. In this approach we implement virtual screening—a computational analog of biological screening. In the virtual screening method, libraries of compounds are searched to verify their potential to bind to specific sites on target molecules—proteins or nucleic acids. Afterwards, well-matched compounds could be tested and the in vitro binding affinity measured.

In this work, such a search was carried out to find potential macromolecular targets for six pentacyclic oxindole alkaloids: isomitraphylline (**1**), isopteropodine (**2**), mitraphylline (**3**), pteropodine (**4**), speciophylline (**5**), and uncarine F (**6**). Reverse virtual screening TarFisDock and ReverseScreen3D web servers were used for initial selection of potential targets. Other possible targets were selected based on literature search and subsequently added to the ones selected by reverse screening servers. Eventually, the alkaloids were docked into their possible targets using molecular docking packages AutoDock 4.2 [15] and AutoDock Vina [16]. Obtained docking results were then used to gain insight into possible interactions of the alkaloids with selected proteins. Molegro Virtual Docker (MVD) was used to evaluate, rescore, and compare crystallized ligand–protein complexes with complexes obtained from AutoDock and Vina by means of ligand–protein energy interactions [17]. MVD applies a heuristic search algorithm that combines differential evolution with a cavity prediction algorithm and a scoring function which is an extended piecewise linear potential (PLP).

Results and discussion

To facilitate identification of the protein targets for alkaloids **1**–**6**, we collated literature data where the anticancer activity of isolated alkaloids against various cancer cell lines were established [29–32]. This limited dataset indicated that mitraphylline (**3**) is the most potent alkaloid. In the in vitro studies, isomitraphylline (**1**) did not show any cytotoxic activity against the studied cancer cell lines. Results of these cytotoxicity assays are summarized in Table 1.

Reverse virtual screening results

The structural information of all alkaloids was submitted to TarFisDock and ReverseScreen3D servers. Unsurprisingly, the results of different screening methods did not indicate one specific protein target. It is thus a challenging task to directly compare results obtained with TarFisDock and ReverseScreen3D (3D search) as they use different databases of molecules and have different strategies in performing search. The 2D searches performed by BindingDB and ReverseScreen2D gave similar results, as in both methods obtained compounds are ranked according to the maximum Tanimoto similarity to structures used as a query. However, due to the fact that *U. tomentosa* alkaloids are stereoisomers, outcomes from 3D searches should provide more relevant information. The list of 54 potential targets was created by combining the results from various screenings and by taking into consideration state-of-the-art articles which indicated the possible mechanism of alkaloids activity. The preferable targets were human proteins whose crystal structures were obtained using X-ray diffraction with high resolution—no lower than 3 Å. This condition was not met once only (tubulin, PDB ID 1sa0). Therefore, it should be noted that, even though the Potential Drug Target Database (PDTD) contains only a limited number of entries which are screened by TarFisDock, the majority of the entries are of high resolution and quality. Furthermore, for some targets selected using the literature search, only a limited number of PDB structures are available.

Consequently, the total number of selected proteins was set to be 69, representing 54 different proteins (see Electronic Supplementary Material). This pool of targets was constructed, and it represented a comprehensive set of kinases and other regulatory proteins which can be implicated in the proapoptotic effects of the alkaloids in question. It was considered to be appropriate for subsequent molecular docking.

AutoDock docking results

Docking of the biologically active alkaloids **1**–**6** into 69 protein targets did not indicate clearly which target is responsible for the cytotoxic effect of these compounds. It can be seen that, even though the structures of the tested molecules resemble each other well, even a small difference in conformation can influence the interactions

Table 1 Cytotoxic activity (activity/μg cm^{-3}) of pentacyclic oxindole alkaloids against multiple cancer cell lines

Cell line	Isopteropodine	Mitraphylline	Pteropodine	Speciophylline	Uncarine F
SK-MEL [29]	>135.0		>135.0	81.0	
KB [29]			>135.0	94.5	
BT-549 [29]			>135.0	91.8	
SK-OV3 [29]	>135.0		100.0	81.0	
VERO [29]			>135.0	105.0	
MHH-ES-1 [30]		17.1			
MT-3 [30]		11.8			
GAMG [31]		20.0			
SKN-BE [31]		12.3			
HL60 [32]					21.7
U-937 [32]					29.0

Reference articles are shown in brackets

between these agents and amino acid side chains in the active sites of proteins.

All the dockings were run using the same settings, and the protein active sites were of the same binding box volume. Nevertheless, the proteins differed in resolution (1.60–3.58 Å), which may have an impact on the docking scores. Bearing all these factors in mind, binding energies were correlated to the values of IC_{50} from in vitro studies on neoplastic cell lines [29–32].

All of the relevant binding scores as calculated by AutoDock are presented in Table 2. Data presented in Table 2 show that proteins with PDB entries 2uw9 (ALK 2), 3iw4 (protein kinase C α), 1hs6 (leukotriene A4 hydrolase), 1sa0 (tubulin), 1tub (tubulin), 1eh4 (casein kinase-1), and 1dhf (dihydrofolate reductase) are the most probable targets when these docking results are studied.

Tubulin has been analyzed in depth over the years and is well known as an anticancer drug target. This protein is overexpressed in neoplastic cells [33, 34]. It should be taken into consideration, however, that the shortcoming of this result is the fact that one of two tubulin files—1sa0—has the lowest resolution of all the downloaded macromolecules. Leukotriene A4 hydrolase is the enzyme that is critical for the production of leukotriene B4. It is one of the key enzymes in inflammation process, yet the inhibition of this enzyme may play a role in cancer prevention and therapy as was indicated by Chen X. et al [35]. Other potential targets have also been reported to play a major role in growth of cancer cells [36, 37]. Each of these proteins is overexpressed in cancer lines.

We tried to identify the most likely target of the selected ligands by employing the approach used previously [14] by correlating the binding scores and biological activity, however this was not viable since a comprehensive dataset to cover all the cell lines was not available. Furthermore, the viability and correctness of studies of isolated alkaloid activities can be questioned due to their recently confirmed property to isomerize [38].

AutoDock Vina docking results

Similarly to AutoDock calculations, the Vina results indicate that alkaloids could be implicated in interactions with several receptors rather than with one single target. As can be seen in Table 3, proteins with IDs 1dhf (dihydrofolate reductase), 3cbx (Dvl-2), 3cqw (Akt-1), 3mpm (Lck), and 1hs6 (leukotriene A4 hydrolase) are indicated as potential targets for the pentacyclic oxindole alkaloids. Methotrexate and pemetrexed are inhibitors of dihydrofolate reductase and act as antimicrobial and anticancer drugs. The biological role of leukotriene A4 hydrolase has been described in the previous section. Akt-1 is a known oncogene, and several active molecules inhibiting this kinase are currently on the market. Most of them, however, do not compete with ATP for the place in the binding pocket [39, 40]. Lck is a tyrosine kinase that is found in immune system cells. Research is being carried out on novel inhibitors of this enzyme [41]. Not much data are available on novel moieties that interact with Dvl-2 protein.

Comparison of docking results

The two software packages used in the study indicated different subsets of proteins, and therefore we carried out a direct comparison of the binding energies of ligand–protein complexes obtained by AutoDock and Vina. For each of 54 selected proteins, the average energy score was calculated from six energy scores of the alkaloid–protein complex, thus creating two separate sets of 54 scores for AutoDock and Vina. Ultimately, the overall score was derived as the average of the two energy scores. In this way, proteins are classified by the overall energy score, where lower energy places the protein higher in the ranking. The ranking of the best ten proteins as classified according to the rescored energies is presented in Table 4.

The binding energies indicate that dihydrofolate reductase could be the most favored target for the alkaloids. It is

Table 2 The five best AutoDock energy scores (kJ mol^{-1}) for each alkaloid

Rank	ID	**1**	ID	**2**	ID	**3**	ID	**4**	ID	**5**	ID	**6**
1	2uw9	−45.1	2uw9	−39.3	1hs6	−40.9	1sa0	−38.6	1tub	−49.6	3iw4	−40.3
2	1eh4	−40.0	1eh4	−39.1	3iw4	−40.5	1dhf	−38.5	1eh4	−38.9	1eh4	−39.4
3	3kvw	−39.9	3oxz	−38.0	3mpm	−39.9	2etr	−37.9	1qpj	−38.6	2uw9	−38.6
4	3fh5	−39.6	1dhf	−37.8	3fh5	−39.2	1byg	−37.4	3cbx	−38.2	1sa0	−38.6
5	3o96	−39.5	1sa0	−37.5	1sa0	−39.1	2uw9	−37.0	1t46	−38.2	3cbx	−38.3

ID protein PDB entry, ***1*** isomitraphylline, ***2*** isopteropodine, ***3*** mitraphylline, ***4*** pteropodine, ***5*** speciophylline, ***6*** uncarine F

Table 3 The five best AutoDock Vina energy scores (kJ mol^{-1}) for each alkaloid

Rank	ID	**1**	ID	**2**	ID	**3**	ID	**4**	ID	**5**	ID	**6**
1	3cbx	−43.3	3o96	−43.3	1hs6	−43.3	3mpm	−43.3	1dhf	−43.3	3cqw	−43.3
2	1hs6	−43.3	1dhf	−43.3	1dhf	−43.3	3cbx	−43.3	3cbx	−43.3	1dhf	−43.3
3	3mpm	−41.2	3cbx	−41.2	3o96	−41.2	1dhf	−41.2	1o6l	−41.2	1hs6	−41.2
4	3kvw	−41.2	1hs6	−41.2	3fh5	−41.2	2pvf	−41.2	1hs6	−41.2	3cbx	−41.2
5	3o96	−40.7	3mpm	−40.7	3iw4	−40.7	1hs6	−40.7	1sa0	−40.7	1sa0	−40.7

ID protein PDB entry, ***1*** isomitraphylline, ***2*** isopteropodine, ***3*** mitraphylline, ***4*** pteropodine, ***5*** speciophylline, ***6*** uncarine F

Table 4 Overall average energy scores (kJ mol^{-1}) for complexes with selected proteins

Protein name	Overall score
Dihydrofolate reductase (ID 1dhf)	−39.6
Dvl-2 (ID 3cbx)	−39.1
Akt-2 (ID 2uw9)	−38.7
Leukotriene A4 hydrolase (ID 1hs6)	−38.2
Akt-2 (ID 1o6l)	−38.1
Tubulin (ID 1sa0)	−37.3
Akt-1 (ID 3cqw)	−37.7
PKC α (ID 3iw4)	−37.0
Lck (ID 3mpm)	−36.9
CK 1 (ID 1csn)	−36.8

followed by Dvl-2, the protein that plays a role in the Wnt signaling pathway. The possible shortcomings of evaluation of this protein due to the lack of experimental data were mentioned above. Akt-2 and leukotriene A4 hydrolase are other targets worth considering in the future. Data mining studies have not indicated Akt-2 as a potential target, as the correlation between in vitro and docking results is low. Leukotriene A4 hydrolase should be studied thoroughly as a potential target for antiinflammatory agents including alkaloids of *U. tomentosa* when their antiinflammatory properties are investigated [42, 43].

Proposed interactions with dihydrofolate reductase

Dihydrofolic acid reductase is the enzyme involved in the conversion of dihydrofolic acid to tetrahydrofolic acid. The latter substance is necessary to synthesize purines and thymine. Reductase is present in all organisms and is essential for life. Due to its importance in cell proliferation and division, it has become a target for anticancer and antimicrobial drugs [44, 45]. The best known drug which inhibits dihydrofolic acid reductase is methotrexate [44, 46, 47]. Another drug that inhibits dihydrofolate reductase is pemetrexed [48].

The most favorable pose of mitraphylline (**3**), the most potent alkaloid in the series, was compared with the binding mode of folic acid in the binding pocket of dihydrofolate reductase (Fig. 2). It can be seen that the native ligand of the enzyme creates several hydrogen bonds. The folate molecule consists of polar pteridine and glutamate moieties that are linked by a rather nonpolar benzoyl ring of PABA group (Fig. 3a). These two aromatic moieties are perpendicular to each other. Mitraphylline (**3**) creates one hydrogen bond to Tyr131 as fewer H-bond donors exist within this molecule. Its binding mode differs as folic acid is a bigger compound.

To further investigate and compare the two dihydrofolate reductase ligands, the rescoring function of MVD was applied. The ligand–protein complex interaction energies for these two complexes are as follows: −535.5 kJ/mol for mitraphylline–dihydrofolate reductase and −584.2 kJ/mol for folic acid–dihydrofolate reductase. It should be taken into consideration that the hydrogen bond energies account for the majority of the calculated 48.7 kJ/mol difference [−11.76 kJ/mol for mitraphylline (**3**) and −46.2 kJ/mol for folic acid]. Similarity between two molecules can indicate similarity in their activities [49]. We calculated the

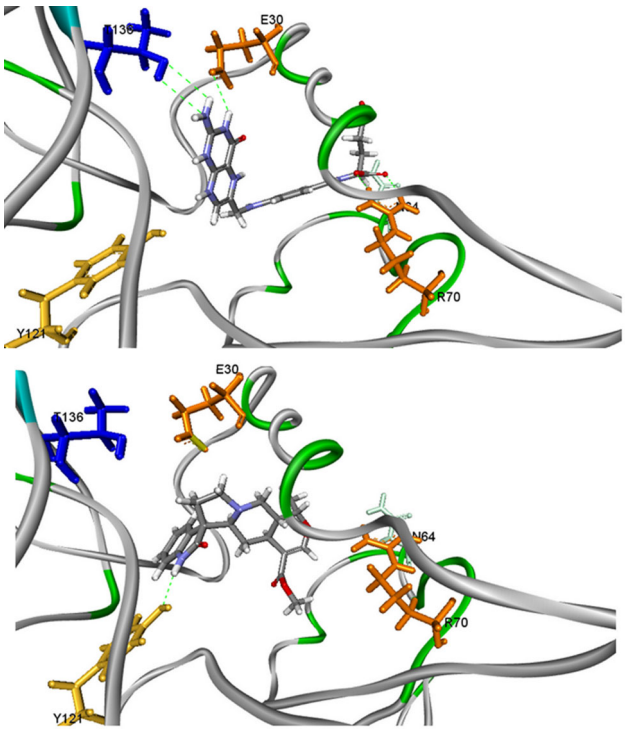

Fig. 2 Mitraphylline (**3**) (*below*) and folate (*above*) as bound in the binding pocket of dihydrofolate reductase. Important residues are depicted, and hydrogen bonds are presented as *green dashed lines*. Carbon atoms are depicted in *black*, oxygen atoms in *red*, nitrogen atoms in *blue*, and hydrogen atoms in *white*. Amino acid colors are used to distinguish between them (color figure online)

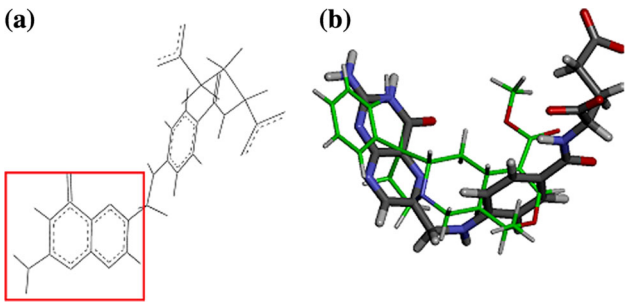

Fig. 3 Folic acid molecule with pteridine moiety indicated within *red box* (**a**) and overlay of folic acid taken from the X-ray structure (PDB entry 1dhf) and a conformation of mitraphylline (**3**) (**b**) (color figure online)

similarity between the two molecules by vROCS, and the Tanimoto combo index was 0.596. The alignment of the two molecules shows similarity of the shape and similar orientation of hydrogen-bond donors and acceptor (Fig. 3b). This alignment is not in agreement with the predicted docked pose; however, both ligands are relatively small compared with the size of the binding pocket. This could lead to multiple binding modes of the smaller ligand, i.e., mitraphylline (**3**). Consequently, judging by the properties of the binding poses, the binding energies of the two studied complexes, and the molecular similarity, it can be pointed out that there is a strong indication that mitraphylline (**3**) and the other pentacyclic oxindole alkaloids will be able to anchor to the binding pocket of the reductase. However, further investigation is needed.

Another docking was run in Vina to verify the high affinity of the alkaloids to the reductase. The dihydrofolate reductase crystal structure file used so far was taken from a 20-year-old study. Thus, it may not possess some information, thus implying errors. The structure file 3ntz (X-ray resolution 1.35 Å) was downloaded and prepared as the other files in this study. This dihydrofolate reductase structure is the most recently solved one, presented as a .pdb file. The Vina docking parameters were set as stated before. The docking scores presented in Table 5 are comparable to those for 1dhf. This further indicates dihydrofolate reductase as the possible target.

Pentacyclic oxindole alkaloids as proposed inhibitors of MDM2

Although the docking of alkaloids exhibits poorer binding scores with MDM2 (for IDs 3lbl and 3jzk, the average binding scores are −30.7 and −31.9 kJ/mol, respectively), we considered it as a potential target important for their activity. MDM2 is a ligase that binds to and inhibits the p53 protein, a very important tumor suppressor that acts inside the cell. The activity of MDM2 is regulated by the activity of p53, and at the same time MDM2 can downregulate p53 in a negative feedback loop. Therefore, MDM2 has been investigated as a potent target for antitumor lead compounds, as described previously in this work. Spiro-oxindole and isoindolinone moieties have recently been reported to exhibit upper-standard potency in in vitro studies [50–53]. The resemblance between these structures and the oxindole ring of the alkaloids **1**–**6** results in a 2D Tanimoto coefficient of similarity of 0.67 by BindingBD. It is the oxindole and indolinone ring that is regarded to be the scaffold that enables the compound to successfully interact with and destabilize the MDM2—p53 complex. Some of the recently investigated structures are shown in Fig. 4 [52].

The binding site conformations of mitraphylline (**3**) and compound **7** [52], which exhibited the highest inhibitory properties in the study by Watson et al., as predicted by Vina, are shown in Fig. 5. It is believed that the modest binding score as stated opens opportunities for design of alkaloid analogs as potential lead molecules.

Interaction with protein tyrosine kinase (PTK)

It has been mentioned in this work that pentacyclic oxindole alkaloids of *U. tomentosa* can possibly interact with PTK [8] in ATP binding site and in this way exhibit their

Table 5 Vina energy scores (kJ mol^{-1}) for alkaloids as bound to dihydrofolate reductase (entry 3ntz)

Alkaloid name	Docking score
Isomitraphylline	−38.2
Isopteropodine	−38.2
Mitraphylline	−37.8
Pteropodine	−39.1
Speciophylline	−41.2
Uncarine F	−36.5

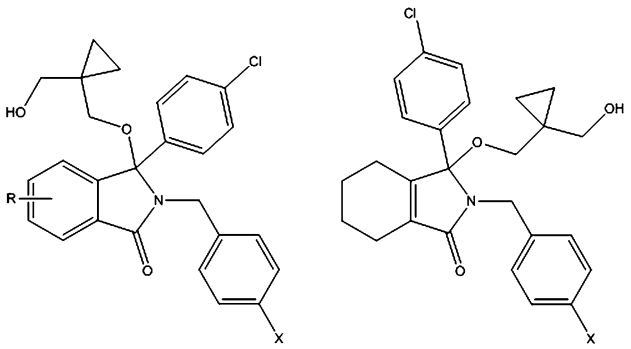

Fig. 4 Isoindolinone structures as investigated recently by Watson et al. *Dextro*- and *levo*-rotatory enantiomers with X = NO_2, CN, and Br were investigated in the cited study

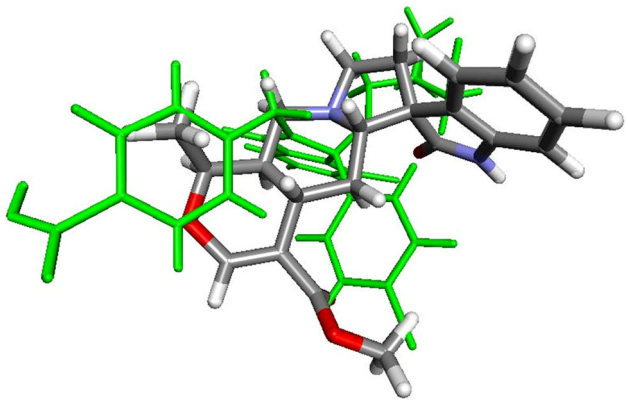

Fig. 5 Poses of mitraphylline (**3**) and **7** (*green sticks*) in the p53 groove on the MDM2 surface. The Vina docking scores for these ligands are −31.9 and −39.9 kJ/mol, respectively (color figure online)

proapoptotic potential. It should be noted that PTK is not a single enzyme; rather, the term is used to describe all the members of this large family of kinases. The authors detected the phosphorylated proteins in the cell to investigate the potential inhibition of PTK (more than 90 tyrosine kinases are known to date) [54], understood as a group of enzymes. There is no doubt that the alkaloids resemble the ATP structure, and therefore their interaction with a tyrosine kinase may occur in the ATP binding site of

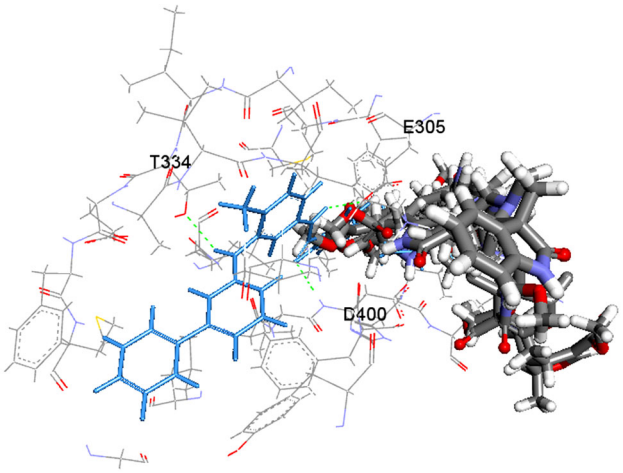

Fig. 6 Poses of superimposed alkaloids and imatinib (*light blue sticks*, query STJ) in the ATP binding pocket of Abl kinase (*lines*). No similarity is seen here, as the compounds are bound differently. Amino acid side chains that form hydrogen bonds with imatinib are shown as *green dashed lines* (color figure online)

an enzyme. However, the particular kinase whose activity was inhibited by the alkaloids was not specified. This is consistent with our findings that do not indicate one specific tyrosine kinase (if any) to be a preferable target in the group of the tyrosine kinases.

Fair results were obtained for Akt-2, Abl, or Lck kinases, but they are not comparable to those calculated for dihydrofolate reductase and MDM2. Example docking poses of the alkaloids and the pose of the crystallized inhibitory molecule imatinib (a very potent inhibitor with market name Gleevec) in the ATP binding pocket of Abl kinase (query 3k5v) are shown in Fig. 6. Note that the binding poses of the given compounds differ as the alkaloids do not overlay with the drug, which occurs mainly due to the differences of the sizes of the molecules. It was reported that the amino acids in the ATP pocket presented in Fig. 6 are of great importance when the inhibitory properties of a ligand are considered [55].

Prevalidation of docking results

The results of our prevalidation reverse screening studies are presented in Table 6. The results indicate that ReverseScreen3D performed better than PharmMapper; however, it cannot be stated that servers predicted the targets with good accuracy. It has to be remembered that the sizes of the compounds and their flexibility affect the scores. These results confirm that only a combination of different computational methods supported by extensive literature search can lead to usable results of in silico target identification that can later guide experimental target validation.

Table 6 Results of reverse screening for ligands with known targets (Electronic Supplementary Material)

Ligand	Known target	RS3D predicted top target	RS3D rank of known target	PM predicted top target	PM rank of known target
CHEMBL1241688	Bcr-Abl kinase	cAMP-specific 3′,5′-cyclic phosphodiesterase 4A	614	Carbonic anhydrase 2	–
Imatinib	Bcr-Abl kinase, Src, Syk	Tyrosine protein kinase Src	13, 1, 3	Proto-oncogene tyrosine protein kinase ABL1	1, 3, 8
CHEMBL483847	Bcr-Abl kinase	Proto-oncogene tyrosine protein kinase ABL1	1	Proto-oncogene tyrosine protein kinase LCK	–
CHEMBL63786	EGF-R kinase	UDP-*N*-acetylglucosamine 1-carboxyvinyltransferase	106	Proto-oncogene tyrosine protein kinase LCK	29
CHEMBL35820	EGF-R kinase	Fructose-1,6-bisphosphatase	4	cAMP-specific 3,5-cyclic phosphodiesterase 4D	–
CHEMBL53711	EGF-R kinase	Cetyl-COA carboxylase	33	Basic fibroblast growth factor receptor 1	44
CHEMBL429743	VEGFR2	Vascular endothelial growth factor receptor 2	1	Vascular endothelial growth factor receptor 2	1
CHEMBL1254007	VEGFR2	B-RAF proto-oncogene serine/threonine protein kinase	5	Vitamin D3 receptor	4
CHEMBL195218	VEGFR2	Mitogen-activated protein kinase 14	138	Vascular endothelial growth factor receptor 2	1
BX-2819	Hsp90	Phosphatidylinositol-4,5-bisphosphate 3-kinase catalytic subunit gamma isoform	4	GTPase HRas	32
Isopropyl analog 5 of BX-2819	Hsp90	B-RAF proto-oncogene serine/threonine protein kinase	8	Sex hormone-binding globulin	24
Ethyl carbamate analog of BX-2819	Hsp90	Phosphatidylinositol-4,5-bisphosphate 3-kinase catalytic subunit gamma isoform	77	3-Phosphoinositide-dependent protein kinase 1	102
CHEMBL181248	Estrogen receptor	Estrogen receptor	1	Cellular retinoic acid-binding protein 2	2
Lasofoxifene	Estrogen receptor	Estrogen receptor	1	Estrogen-related receptor gamma	1
CHEMBL68055	Estrogen receptor	Estrogen receptor	1	Vitamin D3 receptor	2
CHEMBL281957	Tyrosine receptor Src	MAP kinase-activated protein kinase 2	30	Proto-oncogene tyrosine protein kinase ABL1	–
RU84687	Tyrosine receptor Src	Proto-oncogene tyrosine protein kinase Src	1	3-Histone mRNA exonuclease 1	2
CHEMBL421024	Tyrosine receptor Src	Phosphatidylinositol-4,5-bisphosphate 3-kinase catalytic subunit gamma isoform	15	Cellular retinoic acid-binding protein 2	102
Nilotinib	Bcr-Abl kinase, SYK kinase	Tyrosine protein kinase Src	13, 3	Proto-oncogene tyrosine protein kinase LCK	9, 15
Lapatinib	EGFR	Calmodulin-domain protein kinase 1	2	Cellular retinoic acid-binding protein 2	4
Podophyllotoxin	Tubulin	Tubulin beta chain	1	GTPase HRa	–
Geldanamycin	Hsp90	Succinate dehydrogenase hydrophobic membrane anchor protein	12	Peptidylprolyl *cis–trans* isomerase FKBP1A	28
Sunitinib	RET kinase, ITK	Serine/threonine protein kinase NEK2	4, 7	Heat shock protein HSP 90-alpha	–
Olaparib	Tankyrase 2 (poly ADP ribose polymerase)	Poly(ADP-ribose) polymerase 3	1	Cellular retinoic acid-binding protein 2	67

Reverse screening was carried out by ReverseScreen3D (RS3D) and PharmMapper (PM) servers

Conclusions

The extracts of the Amazonian plant *U. tomentosa* contain pentacyclic oxindole alkaloids which exhibit cytotoxic activity in vitro. In this study we tried to identify the potential macromolecular targets for these alkaloids by means of computational studies. In the first step, reverse screening was carried out to build a list of possible targets. The proteins selected by the reverse virtual screening technique were then used for docking of the six pentacyclic oxindole alkaloids **1**–**6**. Using this procedure and judging by its results, we were able to establish that dihydrofolate reductase and MDM2 are the most likely molecular targets for these compounds. However, it has to be noted that reverse screening identified possible interactions with proteins that play a role in the Wnt signaling pathway and possible modulation of oxidative stress, which in turn could also contribute to the overall activity of the alkaloids. Our results suggest that these alkaloids target multiple proteins to exert activity on various cancer cells. Analysis of ligands' conformations obtained using the docking approach shows that mitraphylline (**3**) fits well in the binding site of the reductase and partly mimics the pose of the native ligand. Recent developments in studies on indole ring derivatives that play a role in inhibition of the MDM2–p53 complex support the statement that pentacyclic oxindole alkaloids can possibly interact with MDM2. The results also suggest that the alkaloids could interact with ATP binding pockets of tyrosine kinases, but there is no single enzyme within this group of proteins preferred by these natural products. The computational chemistry approach is therefore thought to be a valuable tool in studies of the biological activity of natural products and can be considered as a good starting point for design of further experiments. It should also be noted that computational approaches require experimental validation, such as NMR spectroscopy, and in vitro investigations using specific targets and cell cultures.

Materials and methods

Preparation of ligand molecules

Alkaloid structures were drawn using ChemBioDraw and saved in .mol2 file format. The files were then opened in Avogadro (an open-source molecular builder and visualization tool, version 1.0.1, http://avogadro.openmolecules.net/), and protons were added for blood pH 7.4. In VEGA ZZ [18] single-point Ammp energy minimization and then systematic conformational search were run to optimize the energies. Afterwards, MOPAC AM1 [19] semiempirical calculations were run. The final conformations of the molecules were produced using ab initio calculations. The DFT/B3LYP6-311G** basis set was used to optimize molecules with the quantum mechanics package NWCHEM [20] and graphical user interface ECCE [21].

Selecting a target pool

The TarFisDock server was set to search through a whole Potential Drug Target Database (http://www.dddc.ac.cn/pdtd/) consisting of 1,207 entries and to output the best top 10 % energy scores for ligand—target complexes. Dock 4.0 [22] provides the basis for the search algorithm and the scoring function used in TarFisDock. Targets categorized as "neoplastic disease" or for which related disease is cancer were chosen along with protein kinases for further analysis.

Ligand-based search through the RCSB Protein Data Bank was carried out using ReverseScreen3D server. Minimized structures of the six pentacyclic oxindole alkaloids (**1**–**6**) obtained using VEGA ZZ were used as query ligands. Both 2D and 3D similarity searches were performed. The best scored ligands from 2D search were used in a subsequent 3D search. Three-dimensional alignments with similarity scores better than 0.4 were taken into account for protein kinases and receptors critical to apoptosis.

BindingDB [23], similarly to ReverseScreen3D, was used to look for similar known ligands with proven activity and for the most common protein tyrosine kinases, judging by IC_{50} data. "Tyrosine kinase", "protein tyrosine kinase", "tyrosine protein kinase", "protein tyrosine", and "ptk" were the entered phrases. The similarity level was set to be greater than 0.6. Ultimately, the RCSB PDB was used to find PDB files of the proteins that take part in the Wnt signaling pathway (Dvl proteins and GSK3β).

Preparation of target molecules

Selected proteins were downloaded from the Protein Data Bank and then checked in Swiss PDB Viewer for possible missing side chains and residues. Hydrogen atoms and charges were added and the whole structure minimized in the Maestro protein wizard suite. If a protein file had several identical subunits, only one of them was taken into consideration. The binding sites of the proteins were identified using either the position of co-crystallized ligand or by the online tool Pocket-Finder (http://www.modelling.leeds.ac.uk/pocketfinder). The volume of the binding site was set to be 22.5 × 22.5 × 22.5 $Å^3$. The size of the binding size is adequate to accommodate ligands and to proceed with the search for an optimal pose.

Molecular docking

Calculations were carried out using two docking programs. AutoDock 4.2 is an automated docking suite capable of performing rigid or flexible docking [15]. AutoDock is one of the most frequently used molecular docking suites and has been extensively validated over the years [24–26]. The AutoDock scoring function is based on the AMBER force field, while a Lamarckian genetic algorithm is implemented for finding best poses. The settings for the program used in this study were as follows: 100 runs with 2,500,000 energy evaluations and a maximum number of 27,000 generations. This resulted in 100 solutions assessed by binding scores.

The AutoDock Vina [16] software was released in 2009, and was also employed in this work. Vina has been used widely in recent years, with recent evaluation being reported in February 2013 [27]. The empirical scoring function and the iterated local search for global optimization were employed here to achieve a significantly improved calculation speed and better efficiency compared with AutoDock. The default settings for docking in Vina were used except for num_modes (20) and exhaustiveness (100).

To combine results from AutoDock and AutoDock Vina, the average score taken from these two docking suites was used, as it is believed to represent a clear and effective way of presenting the results. To further compare our docking results with co-crystallized ligand complexes with selected proteins, the MolDock score from the Molegro Virtual Docker package was implemented [17]. The default settings and the same binding pockets on protein surface were used as for AutoDock and Vina. The ligand evaluation was calculated including internal electrostatic interactions (ES), internal H-bonds, and sp2–sp2 torsions.

Molecular similarity

The conformations of mitraphylline (**3**) were calculated using the OMEGA software package (Omega, v. 2012; OpenEye Scientific Software, Inc., Santa Fe, NM, USA) and saved as .oeb multiple structure file. The resulting structures were aligned by rigid alignment to the conformation of the folic acid taken from the crystal structure of dihydrofolate reductase (PDB entry 1dhf). The molecular similarity was estimated by comparing the shape of two molecules using vROCS (vROCS, v. 2011; OpenEye Scientific Software, Inc., Santa Fe, NM, USA).

Validation of the reverse virtual screening method

To validate the virtual screening approach used in this project, we selected a group of several known protein targets along with their three most potent ligands. The selection of ligands was based on IC_{50} values as presented in the BindingDB database. We also selected six molecules that have been introduced into the market (imatinib, nilotinib, lapatinib, axitinib, sunitinib, and olaparib). The screenings were carried out by submitting all molecules to ReverseScreen3D and PharmMapper [28] servers. PharmMapper was created by the same authors as TarFisDock and uses the triangle hashing method to compare pharmacophores based on information on 1,500 drug targets. Both servers were screened through using default settings. The complete list of selected ligands and protein targets is presented in the Electronic Supplementary Material.

Acknowledgments The authors would like to thank Teresa Barata, Ph.D. (The UCL School of Pharmacy) and Michał Łaźniewski (Faculty of Pharmacy, Medical University of Warsaw) for their excellent advice while preparing this publication.

References

1. Reinhard KH (1999) J Altern Complement Med 5:143
2. Keplinger K, Laus G, Wurm M, Dierich M, Teppner H (1999) J Ethnopharmacol 64:23
3. Kang TH, Murakami Y, Matsumoto K, Takayama H, Kitajima M, Aimi N, Watanabe H (2002) Eur J Pharm 455:27
4. De Martino L, Silva Martinot JL, Franceschelli S, Leone A, Pizza C, de Feo V (2006) J Ethnopharm 107:91
5. Gurrola-Diaz CM, García-López PM, Gulewicz K, Pilarski R, Dihlmann S (2011) Phytomed Int J Phytother Phytopharm 18:683
6. Pilarski R, Filip B, Wietrzyk J, Kuraś M, Gulewicz K (2010) Phytomed Int J Phytother Phytopharm 17:1133
7. Paradowska K, Wolniak M, Pisklak M, Gliński JA, Davey MH, Wawer I (2008) Sol State Nucl Mag Reson 34:202
8. Berry JP, Laux M, Rodgriguez E (2002) J Med Sci 2:110
9. Hardjito L, Royani DS, Santoso J (2012) J Food Sci Eng 2:550
10. Pilarski R, Gurrola-Díaz CM, García-López PM, Soldevila G, Olejnik A, Grajek W, Gulewicz K (2013) J Herb Med 3:149
11. Dreifuss AA, Bastos-Pereira AL, Fabossi IA, Lívero FA, Stolf AM, Alves de Souza CE, Gomes Lde O, Constantin RP, Furman AE, Strapasson RL, Teixeira S, Zampronio AR, Muscará MN, Stefanello ME, Acco A (2013) PLoS One 8:e54618
12. Gao Z, Li H, Zhang H, Liu X, Kang L, Luo X, Zhu W, Chen K, Wang X, Jiang H (2008) BMC Bioinf 9:104
13. Kinnings SL, Jackson RM (2011) J Chem Inf Model 51:624
14. Eric S, Ke S, Barata T, Solmajer T, Antić Stanković J, Juranić Z, Savić V, V, Zloh M (2012) Bioorg Med Chem 20:5220
15. Morris GM, Goodsell DS, Halliday RS, Huey R, Hart WE, Belew RK, Olson AJ (1998) J Comp Chem 19:1639
16. Trott O, Olson AJ (2010) J Comp Chem 31:455
17. Thomsen R, Christensen MH (2006) J Med Chem 49:3315
18. Pedretti A, Villa L, Vistoli G (2004) J Comp-Aided Mol Des 18:167
19. Stewart JJ (1990) J Comp-Aided Mol Des 4:1
20. Valiev M, Bylaska EJ, Govind N, Kowalski K, Straatsma TP, van Dam HJJ, Wang D, Nieplocha J, Apra E, Windus TL, de Jong WA (2010) Comput Phys Commun 181:1477
21. Black GC, Chatterton J, Daily J, Elsethagen T, Feller D, Gracio D, Jones D, Keller T, Lansing C, Matsumoto S, Palmer B, Peterson M, Schuchardt K, Stephan E, Sun L, Swanson K, Taylor H,

Thomas G, Vorpagel E, Windus T, Winters C (2009) ECCE, a problem solving environment for computational chemistry, software version 6.0. Pacific Northwest National Laboratory, Washington, pp 99352–100999
22. Ewing TJ, Shingo MA, Skillman G, Kuntz ID (2001) J Comp-Aided Mol Des 15:411
23. Liut T, Lin Y, Wen X, Jorissen RN, Gilson MK (2007) Nucl Acid Res 35:198
24. Alia H, Ashidab N, Nagamatsua T (2008) Bioorg Med Chem Lett 18:922
25. Mulakala C, Nerinckx W, Reilly PJ (2006) Carbohydr Res 341:2233
26. Xiao ZP, Ma TW, Fu WC, Peng XC, Zhang AH, Zhu HL (2010) Eur J Med Chem 45:5064
27. Gathiaka S, Nanayakkara G, Boncher T, Acevedo O, Wyble J, Patel S, Patel A, Shane ME, Bonkowski B, Wieczorek J, Rong Y, Huggins K, Smith F, Amin RH (2013) Bioorg Med Chem Lett 23:873
28. Xiaofeng L, Ouyang S, Yu B, Liu Y, Huang K, Gong J, Zheng S, Li Z, Li H, Jiang H (2010) Nucl Acid Res 38:W609
29. Muhammad I, Dunbar DC, Khan RA, Ganzera M, Khan IA (2001) Phytochemistry 57:781
30. Garcia Gimenez D, García Prado E, Sáenz Rodríguez T, Fernández Arche A, De la Puerta R (2010) Planta Med 76:133
31. Garcia Prado E, García Gimenez MD, De la Puerta Vázquez R, Espartero Sánchez JL, Sáenz Rodríguez MT (2007) Phytomed Int J Phytother Phytopharm 14:280
32. Stuppner H, Sturm S, Geisen G (1993) Planta Med 59:A593
33. Lesyk R, Zimenkovsky B, Atamanyuk D, Jensen F, Kieć-Kononowicz K, Gzella A (2006) Bioorg Med Chem 14:5230
34. Novoa A, Pellegrini-Mose N, Bourg S, Thoret S, Dubois J, Aubert G, Cresteil T, Chapleur Y (2011) Eur J Med Chem 46:3570
35. Chen X, Wang S, Wu N, Yang CS (2004) Curr Cancer Drug Targets 4:267
36. Goldstein DR, Cacace AM, Weinstein IB (1995) Carcinogenesis 16:1121
37. Koivunen J, Aaltonen V, Peltonen J (2006) Cancer Lett 235:1
38. Kaiser S, Dietrich F, de Resende PE, Verza SG, Moraes RC, Morrone FB, Batastini AM, Ortega GG (2013) Planta Med 79:1413
39. Gilot D, Giudicelli F, Lagadic-Gossmann D, Fardel O (2010) Chem Biol Interact 188:546
40. Lee CS, Kim YJ, Jang ER, Myung SC, Kim W (2010) Eur J Pharm 632:7
41. Deak HL, Newcomb JR, Nunes JJ, Boucher C, Cheng AC, DiMauro EF, Epstein LF, Gallant P, Hodous BL, Huang X, Lee JH, Patel VF, Schneider S, Turci SM, Zhu X (2008) Bioorg Med Chem Lett 18:1172
42. Grice CA, Tays KL, Savall BM, Wei J, Butler CR, Axe FU, Bembenek SD, Fourie AM, Dunford PJ, Lundeen K, Coles F, Xue X, Riley JP, Williams KN, Karlsson L, Edwards JP (2008) J Med Chem 51:4150
43. Sandoval M, Charbonnet RM, Okuhama NN (2000) Free Radic Biol Med 29:71
44. Schweitzer BI, Dicker AP, Bertino JR (1990) FASEB J 4:2441
45. Banerjee D, Mayer-Kuckuk P, Capiaux G, Budak-Alpdogan T, Gorlick R, Bertino JR (2002) Biochim Biophys Acta 1587:164
46. Gangjee A, Li W, Lin L, Zeng Y, Ihnat M, Warnke LA, Green DW, Cody V, Pace J, Queener SF (2009) Bioorg Med Chem 17:7324
47. Lladó V, Terés S, Higuera M, Alvarez R, Noguera-Salva MA, Halver JE, Escribá PV, Busquets X (2009) Proc Natl Acad Sci U S A 106:13754–13758
48. Adjei AA (2002) Semin Oncol 29:503
49. Drakulic BJ, Stavri M, Gibbons S, Zizak ZS, Verbić T, Juranić IO, Zloh M (2009) Chem Med Chem 4:1971
50. Watson AF, Liu J, Bennaceur K, Drummond CJ, Endicott JA, Golding BT, Griffin RJ, Haggerty K, Lu X, McDonnell JM, Newell DR, Noble ME, Revill CH, Riedinger C, Xu Q, Zhao Y, Lunec J, Hardcastle IR (2011) Bioorg Med Chem Lett 21:5916
51. Hardcastle IR, Ahmed SU, Atkins H, Farnie G, Golding BT, Griffin RJ, Guyenne S, Hutton C, Källblad P, Kemp SJ, Kitching MS, Newell DR, Norbedo S, Northen JS, Reid RJ, Saravanan K, Willems HM, Lunec J (2006) J Med Chem 49:6209
52. Hardcastle IR, Liu J, Valeur E, Watson A, Ahmed SU, Blackburn TJ, Bennaceur K, Clegg W, Drummond C, Endicott JA, Golding BT, Griffin RJ, Gruber J, Haggerty K, Harrington RW, Hutton C, Kemp S, Lu X, McDonnell JM, Newell DR, Noble ME, Payne SL, Revill CH, Riedinger C, Xu Q, Lunec J (2011) J Med Chem 54:1233
53. Sosin AM, Burger AM, Siddiqi A, Abrams J, Mohammad RM, Al-Katib AM (2012) J Hematol Oncol 5:57
54. Robinson DR, Wu YM, Lin SF (2000) Oncogene 19:5548
55. Zhang J, Adrián FJ, Jahnke W, Cowan-Jacob SW, Li AG, Iacob RE, Sim T, Powers J, Dierks C, Sun F, Guo GR, Ding Q, Okram B, Choi Y, Wojciechowski A, Deng X, Liu G, Fendrich G, Strauss A, Vajpai N, Grzesiek S, Tuntland T, Liu Y, Bursulaya B, Azam M, Manley PW, Engen JR, Daley GQ, Warmuth M, Gray NS (2010) Nature 463:501